11

Engineered Heart Tissue

Thomas Eschenhagen and Wolfgang H. Zimmermann

Institute of Experimental and Clinical Pharmacology, University Hospital, Hamburg Eppendorf 20246 Hamburg, Germany

Corresponding author: t.eschenhagen@uke.uni-hamburg.de

Culture of Cells for Tissue Engineering, edited by Gordana Vunjak-Novakovic and R. Ian Freshney

1. BACKGROUND

Cell-based therapies have been suggested as a novel and potentially curative approach for replacement of impaired myocardium [Reinlib and Field, 2000]. Presently, two principally different approaches have been developed: (1) implantation of isolated cells by direct injection into the myocardium or by percutaneous applications [Koh et al., 1993; Soonpaa et al., 1994; Li et al., 1996; Scorsin et al., 1997; Taylor et al., 1998; Reinecke et al., 1999; Sakai et al., 1999; Tomita et al., 1999; Condorelli et al., 2001; Etzion et al., 2001; Menasche, 2001; Orlic et al., 2001; Müller-Ehmsen et al., 2002a,b; Roell et al., 2002] and (2) construction of cardiac muscle constructs in vitro that can be surgically attached to the myocardium [Bursac et al., 1999; Carrier et al., 1999; Leor et al., 2000; Li et al., 2000]. The present article describes our own approach aimed at developing a functional cardiac tissue construct suitable for cardiac replacement therapy.

In 1994, our idea to generate 3-dimensional cardiac tissue constructs came from the observation that it is relatively easy to genetically manipulate cultured immature cardiac myocytes in the classic 2-dimensional culture format (and to observe biochemical or molecular consequences) but difficult to obtain reliable information from these cells in terms of contractile function. Evaluation of contractile consequences of any genetic manipulation would be essential, however, for the validation of potentially relevant genes identified by gene expression arrays that we and others performed at that time.

The description of a method to culture embryonic chick fibroblasts in collagen I in a 3-D format that allowed measurement of (tonic) contractile forces in the organ bath by the group of E. L. Elson [Kolodney and Elson, 1993] stimulated us to adapt the method to embryonic chick cardiac myocytes. The experiments quickly yielded success, and cardiac myocytes spontaneously generated a coherently and regularly beating cardiac tissue-like structure (cardiac myocyte-populated matrix, CMPM) that developed measurable forces when suspended in organ baths and connected to a force transducer [Eschenhagen et al., 1997]. The success was surprising because others had described that cardiac myocytes from neonatal rats do not grow *inside* a collagen I matrix but can only be cultured *on top* of a preformed collagen I matrix [Souren et al., 1992]. We later learned that, indeed, cardiac myocytes from neonatal rats, in contrast to embryonic chick cardiac myocytes, did not spontaneously form a tissuelike structure when cultured in collagen I, but needed supplementation of Matrigel and a modification of the cell-matrix composition in the original reconstitution mixture [Zimmermann et al., 2000].

The initial experimental setup followed the one proposed by E. L. Elson's group in St. Louis and consisted of two glass tubes held at a defined distance by a metal spacer in a rectangular well (Fig. 11.1). When cardiac myocytes were mixed with neutralized liquid collagen I and pipetted between the two glass tubes they yielded biconcave lattices spanning between the glass tubes. Contractile force could easily be measured by transferring CMPMs in an organ bath and suspending the glass tube-anchored lattices between a fixed holder and a force transducer.

What we learned in this system was the importance of mechanical strain. At the free edges, the region of increased strain, cells formed a dense network of muscle bundles that were oriented along the edges, that is, in the direction of the strain (See Fig. 11.1). In contrast, cells formed only a loose and randomly oriented network in the central parts of the lattices (See Fig. 11.1). Thus it appeared as if the orientation of cells reflected the biomechanical strain throughout the lattice. The importance of strain was substantiated by experiments in which CMPMs were subjected to a 5-day cyclic stretch regimen imposed by a motorized device [Fink et al., 2000]. This resulted in a three- to fivefold increase in contractile force development, hypertrophy of cardiac myocytes in CMPMs, and improved tissue formation at the free edges. A systematic analysis of the relation between the degree of stretch and force development showed that the strain had a threshold of approximately 5–7% that was necessary to induce CMPM formation with improved

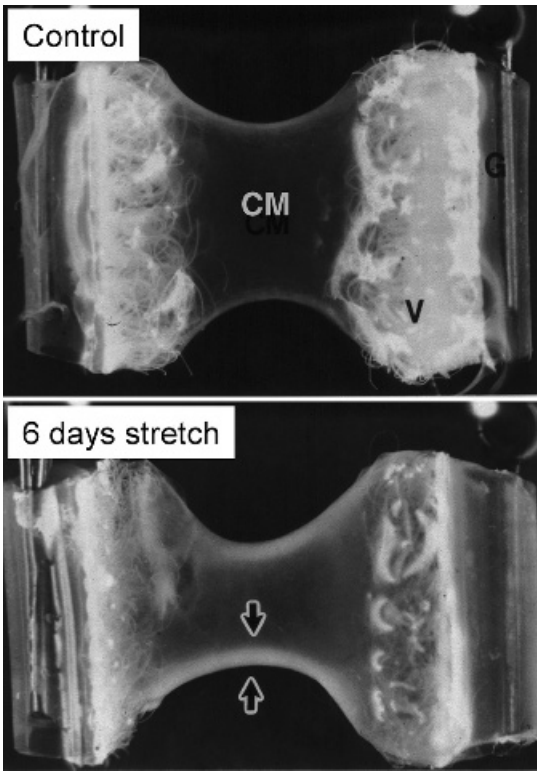

Figure 11.1. Morphology of cardiac myocyte-populated matrix (CMPM) with and without phasic stretch. Note the dense cell population at the free edges and sparse population in the center. After 6-day stretch the cell-rich area increased. Size of CMPM is 15×10 mm. From Fink et al. [2000].

tissue properties [Fink et al., 2000]. Larger strains did not further improve force, and strains higher than 20% tended to disrupt the CMPM structure.

CMPMs proved to be a valuable system to measure pharmacological responses to β-adrenergic and muscarinic agonists and extracellular calcium [Eschenhagen et al., 1997; Fink et al., 2000; Zimmermann et al., 2000] as well to transfer cardiac genes [Most et al., 2001; Remppis et al., 2003]. However, the inhomogeneity of cell orientation and tissue formation and the need for the production of casting devices with Velcro-covered glass tubes led to variable results and motivated us to think about an easier setup. The solution was a ring-shaped casting mold into which the cell-collagen-Matrigel mixture was pipetted. These casting molds are reproducibly produced from silicone in large quantities and can be used indefinitely [Zimmermann et al., 2000, 2002a]. In addition to their practical advantages, the ring-shaped engineered heart tissues (EHTs) had much better tissue homogeneity, likely due to the more homogeneous distribution of biomechanical strain. Circular EHTs have also been utilized to study gene function [El-Armouche et al., 2003; Zolk et al., 2003]. Hence, all our subsequent studies have been carried out with the improved circular EHT system.

With the growing interest in cardiac tissue engineering and the progress made in using embryonic and adult stem cells to derive cardiac myocytes, it became

obvious that EHTs may prove valuable as tissue replacement material. Several questions have been addressed or are under current evaluation.

1.1. Can EHT Contractile Function and Tissue Formation be Improved as Compared to Our Standard Protocol?

Cell density, collagen I content, chick embryo extract, and horse serum requirements have been tested. Cell concentration had a biphasic effect on force development. When cell number per EHT was increased from 0.5 to 2.5 $\times$ 10^6, the force of contraction increased; for cell numbers above 2.5 $\times$ 10^6 cells/EHT the contractions ceased, probably because of metabolic problems. The contractile force was highest for 0.5 and 0.7 mg collagen/EHT and decreased both above and below this range, whereas the mechanical integrity increased with collagen content. The standard collagen content was set to 0.8 mg/EHT [Eschenhagen et al., 2002]. Chick embryo extract appeared not to be essential throughout the duration of culture. In contrast, EHTs depended on the continuous presence of horse serum at 10% v/v (Fig. 11.2). Any reduction of the serum content resulted in a rapid reduction of the contractile activity [Eschenhagen et al., 2002]. Higher serum concentrations have not been tested systematically.

1.2. Do EHTs Survive When Implanted into the Peritoneum of Rats?

Experiments in syngeneic rats showed that EHTs became quickly and strongly vascularized and survived for at least 4 weeks when implanted under the peritoneum [Eschenhagen et al., 2002]. Histology, however, showed infiltration of the EHT by mononuclear cells and multinucleated giant cells, predominantly at the implant periphery. Despite the apparent immune response, cardiac myocytes retained a cross-striated morphology for at least 4 weeks after implantation.

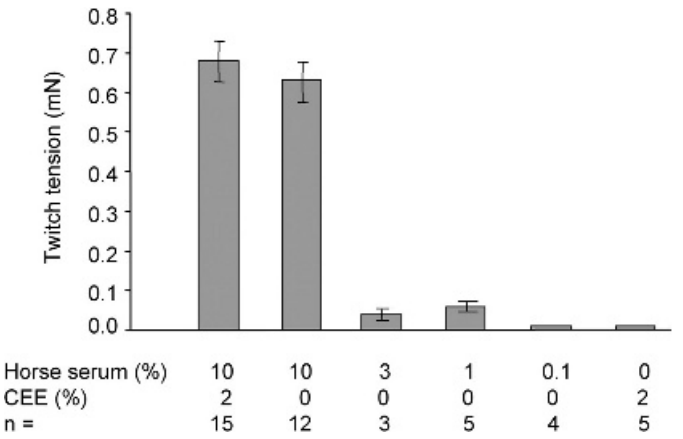

Figure 11.2. Serum dependence of EHT. EHTs were cultured for 7 days in the presence of 10% horse serum (HS) and 2% chick embryo extract (CEE) and for another 5 days in the presence of the indicated concentrations of supplements. The ordinate indicates twitch tension at maximally effective extracellular calcium concentrations in the organ bath. Note that reduction of horse serum reduced twitch tension to almost zero, whereas depletion of chick embryo extract had no effect. From Eschenhagen et al. [2002].

1.3. Do EHTs Survive When Implanted onto the Heart of Rats?

In contrast to implantation into the peritoneum, EHTs did not survive when implanted onto the heart of syngeneic rats [Zimmermann et al., 2002b]. After 2 weeks, we observed a strong immune response with destruction of implanted cardiomyocytes and replacement fibrosis. The difference in the immune responses following EHT implantation in the peritoneum and on the heart is presently unclear. The immune response in general was no surprise. Although collagen and heart cells were carefully isolated from syngeneic rats (Fischer 344) we utilized various xenogeneic components in the original EHT reconstitution mixture and during in vitro maturation: horse serum, Matrigel, and chick embryo extract. Any of these factors might have been the cause of immune activation. A likely explanation is an impregnation of otherwise syngeneic cells with xenogeneic proteins. When the experiments were repeated under immunosuppression with cyclosporine, azathioprine, and methylprednisolone, EHTs survived for up to 8 weeks, continued to contract, and became heavily vascularized and even innervated [Zimmermann et al., 2002b]. Importantly, the examination of myocyte ultrastructure revealed sarcomere development with clear signs of maturation and a regular formation of M-bands that were only rarely seen during cultivation of EHTs in vitro. These data support the hypothesis that the growth factor milieu and/or the cellular environment of adult host myocardium drives cardiac myocytes into terminal differentiation.

1.4. Do EHTs Become Vascularized and Integrate into the Recipient Heart?

As noted above, EHTs quickly become vascularized, both under the peritoneum and on the heart. Blood vessel ingrowth is visible as early as 3 days. After 4 weeks, the entire EHT is penetrated by functional blood vessels, as confirmed by the ultrastructural demonstration of erythrocytes in the blood vessels [Zimmermann et al., 2002b]. We are currently evaluating whether the preformed capillaries and primitive vascular structures that are regularly seen in EHTs during in vitro cultivation [Zimmermann et al., 2002a] participate in vascularization after implantation onto the heart. The relevance of large myelinated and nonmyelinated nerve fibers that have been found in EHTs 4 weeks after implantation remains unknown.

An important question is whether EHTs electrically and functionally integrate into the host myocardium. First series of electrical mapping experiments indicate that electrical coupling of EHT to host myocardium has occurred 4 weeks after implantation onto infarcted rat hearts [Zimmermann et al., 2003]. Mechanical coupling is more difficult to prove because mechanical activity of the EHT, when integrated well in the host myocardium, cannot be differentiated by eye from the beating of the heart. More sophisticated evaluation methods are needed to answer this question.

1.5. Do EHTs Alter the Contractile Function of Uninjured Hearts?

Contractile function of the uninjured hearts did not change after EHT implantation, as demonstrated by echocardiographic analysis [Zimmermann et al., 2002b].

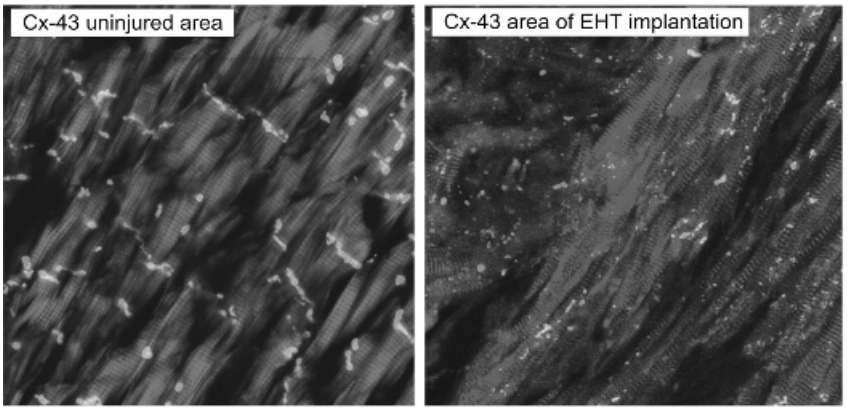

Figure 11.3. Effect of EHT implantation of the spatial organization of connexin 43 (Cx-43) in rat hearts. The left panel shows an immunoconfocal image from the middle of a rat heart, the right panel from the area of EHT implantation (EHT upper left corner, host myocardium right lower part). Cx-43 is indicated in green, phalloidin-stained actin in red. Note the disorganization of Cx-43 at the implantation site. (See Color Plate 6A.)

This may seem trivial, but one could argue that there is some reaction of host myocardium to the implanted EHT that may result in deterioration of contractile function. This could include impairment of diastolic function, which is typically observed in classic dynamic cardiomyoplasty or structural alteration on the cellular level. However, the pattern of spatial connexin 43 distribution at the site of EHT implantation differed from that in uninjured myocardium, as observed by immunochemical staining (Fig. 11.3, See Color Plate 6A). Alterations in connexin 43 immune staining have been previously observed in developing and diseased hearts [Kostin et al., 2002].

1.6. Do EHTs Improve Cardiac Function after Myocardial Infarction?

The most important question is whether implantation of the engineered tissue constructs can improve contractile function after myocardial infarction. We have chosen the model of coronary ligation as being relatively close to human pathology and have set up an experimental model in which the size and the functional consequences of coronary ligation are well defined. Large longitudinal studies using echocardiography, magnetic resonance imaging, and left heart catheterization to analyze in vivo hemodynamics are currently being performed to evaluate the feasibility of our approach.

2. PREPARATION OF REAGENTS

2.1. Complete Culture Medium

Dulbecco's modified minimal essential medium (DMEM) supplemented with 10% horse serum, 2% chick embryo extract, 100 μg/ml streptomycin, and 100 U/ml penicillin G, all sterile, stored at 4 °C for up to 2 weeks.

2.2. Calcium- and Bicarbonate-Free Hanks' Balanced Salt Solution with HEPES (CBFHH)

NaCl 136.9 mM, KCl 5.36 mM, $MgSO_4 \cdot (H_2O)_7$0.81 mM, glucose 5.55 mM, $KH_2PO_4$0.44 mM, $Na_2HPO_4 \cdot (H_2O)_7$0.34 mM, HEPES 20 mM, adjusted to pH 7.5 with NaOH (all chemicals are of analytical grade or best commercially available). Sterilize by filtration.

2.3. Tyrode's Solution (0.2 mM and 0.4 mM Ca^{2+})

NaCl 119.8 mM, KCl 5,4 mM, $MgCl_2$ 1.05 mM, $CaCl_2$ 0.2 mM or 0.4 mM, NaH_2PO_4 0.42 mM, $NaHCO_3$ 22.6 mM, glucose 5.05 mM, Na_2EDTA 0.05 mM, ascorbic acid 0.28 mM. Maintain pH at 7.4 by bubbling with 95% O_2−5% CO_2 (carbogen).

2.4. Trypsin Stock Solution (0.1 g/ml; 50×)

Dissolve 5 g in 50 ml of CBFHH overnight with gentle shaking. Sterilize by filtration. Dilute 1:50 with CBFHH for use.

2.5. DNase Stock Solution (2 mg/ml; 71×)

Dissolve 100 mg in 50 ml of NaCl (0.15 M). Sterilize by filtration and store at −20 °C. Dilute 1 ml with 70 ml of CBFHH for use at 28 μg/ml.

2.6. Concentrated DMEM (2×)

DMEM made up at double strength from powder and filter sterilized, or from 10× concentrate.

2.7. Histologic Fixative

Formaldehyde 4%, methanol 1%, in phosphate-buffered saline (PBS), pH 7.4, containing 1 mM $CaCl_2$ and 30 mM 2,3-butanedione monoxime (BDM).

2.8. Supplemented Tris-Buffered Saline (STBS)

Tris•HCl 0.05 M, NaCl 0.15 M, pH 7.4, containing 10% fetal calf serum, 1% bovine serum albumin, 0.5% Triton X-100, and 0.05% thimerosal.

2.9. Glutaraldehyde Fixative

Glutaraldehyde 2.5% in PBS, pH 7.4 containing 1 mM $CaCl_2$ and 30 mM BDM

3. ISOLATION AND CULTURE METHODOLOGY

The principle of EHT preparation is simple. Freshly isolated neonatal rat heart cardiac myocytes are mixed with freshly neutralized rat tail collagen I, Matrigel® (alternatively Harbor Extracellular Matrix (ECM), which is also extracted from

Engelbreth–Holm–Swarm tumors in mice), and a medium concentrate calculated to yield a final concentration of 1× DMEM, 10% horse serum, and 2% chick embryo extract. This reconstitution mixture is prepared on ice, well mixed by pipetting, and then pipetted into ring-shaped casting molds at room temperature (Fig. 11.4a, See Color Plate 6B). After transfer into the 5% CO_2 incubator at 37 °C the reconstitution mixture quickly (30 min) consolidates, yet remains soft, and thus traps the cells in a geometrically defined 3D environment.

During the first 2–3 days the cells start to spread out, develop cell-cell contacts, and form spontaneously contracting aggregates. Over time aggregates organize into longitudinally oriented strands with diameters of up to 200 μm that become highly interconnected throughout the matrix into a dense muscular 3D network. During the consolidation process EHTs undergo extensive matrix remodeling and change from an initially slack gel that fills the entire circular well (outer/inner diameter: 16/8 mm, height: 5 mm) to a contracted and mechanically stable ring

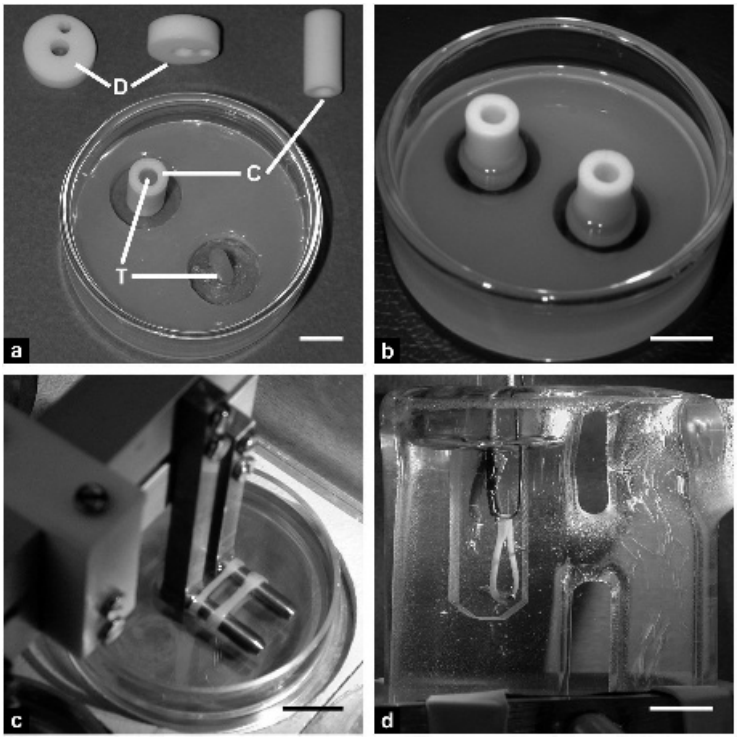

Figure 11.4. Experimental setup for EHT preparation, culture, phasic stretch and analysis of contractile function in the organ bath. a) Casting mold assembly: Silicone tubing (T) was glued to the surface of glass culture dishes. Either Teflon disks (D) or cylinders (C) can be placed over silicone tubing to function as removable spacers during casting mold preparation and EHT culture, respectively. b) EHTs condensed around the central Teflon cylinder in casting molds between culture days 1 and 4. Thereafter, no change of gross morphology was observed. c) EHTs after transfer in a stretch apparatus to continue culture under unidirectional and cyclic stretch (10%, 2 Hz). d) EHT in a thermostatted organ bath. Bars: 10 mm. From Zimmermann et al. [2002a]. (See Color Plate 6B).

(outer/inner diameter: 10/8 mm; thickness: 1 mm) (Fig. 11.4b,c, See Color Plate 6B). During the consolidation process, we transfer EHTs to a stretch device to continue culture under defined phasic strain (10%, 2 Hz) for 5–7 days (Fig. 11.4c, See Color Plate 6B). Under these conditions optimal maturation of EHTs has been observed. Longer periods of stretch often resulted in EHT disruption. Alternatively, EHTs can be cultured under static stretch on simple stainless steel holders, for up to 4 weeks.

3.1. Myocyte Preparation

Cardiomyocytes are isolated from 1- to 3-day-old neonatal rat hearts by a modification of the technique described by Webster et al. [1994].

Protocol 11.1. Isolation of Neonatal Cardiac Myocytes

Reagents and Materials

Sterile

- ❑ Complete medium (See Section 2.1)
- ❑ CBFHH (calcium- and bicarbonate-free HEPES-buffered Hanks' balanced salt solution, pH 7.5, See Section 2.2)
- ❑ Trypsin, 2 mg/ml (See Section 2.4)
- ❑ DNase stock, 2 mg/ml (See Section 2.5)
- ❑ DNase I, working concentration, 28 μg/ml (See Section 2.5)
- ❑ Petri dishes, 15 cm
- ❑ Plastic tube, 50 ml
- ❑ Dissection instruments: scissors, forceps, scalpels
- ❑ Gauze filter: 100-μm mesh

Non-sterile

- ❑ Newborn rat pups

Protocol

(a) Decapitate the pups quickly.
(b) Excise the hearts and remove atria and great vessels.
(c) Keep in 20 ml CBFHH in a 15-cm culture dish at room temperature until all hearts are prepared. For our routine cell isolations, we utilize 30–60 neonatal rat hearts.
(d) Cut the hearts in half.
(e) Wash 3 times with CBFHH.
(f) Mince extensively with scissors in about 5 ml CBFHH to a size of approximately 1 mm^3.
(g) Wash the tissue fragments again in CBFHH.
(h) Transfer to a 50-ml plastic tube for serial trypsin digestion.
(i) Allow tissue fragments to settle and discard the supernate.
(j) Add 10 ml trypsin solution (per total preparation of 30–60 hearts).
(k) Digest at room temperature (~20 °C) for 20 min with gentle agitation.

(l) Allow tissue fragments to settle.
(m) Discard the turbid supernate
(n) Add 9 ml DNase I, 28 μg/ml, to digest traces of DNA that impair sedimentation of tissue fragments and separation from isolated cells. DNase digestion is facilitated by triturating 25 times with a wide-bore pipette.
(o) Allow the tissue fragments to settle, and discard the supernate.
(p) Add 10 ml trypsin for the next cycle of digestion, this time for about 5 min.
(q) Collect the supernates of this trypsin digestion and of the following trituration with DNase I in 50-ml tubes containing 2 ml fetal calf serum (FCS) to inactivate the trypsin, and keep on ice.
(r) Repeat this digestion cycle until nearly complete digestion of the heart tissue is obtained. Over time, gradually reduce the volumes of trypsin and DNase I to 7.5 ml trypsin and 6.5 ml DNase I. After most tissue fragments are disaggregated, the remainder is discarded.
(s) Centrifuge the 50-ml collection tubes (generally 4–6 tubes) at 50 *g* for 15 min at 4 °C, and discard the supernate.
(t) Resuspend the cell pellet in 2 ml complete medium and pool all the pellets in one of the tubes.
(u) Rinse the other tubes with 2 ml medium each and pool.
(v) Add 250 μl DNase I stock solution per 30-ml cell suspension, triturate the suspension 25×, and centrifuge as above.
(w) Discard the supernate and resuspend the cell pellet in 32 ml medium.
(x) Filter the cell suspension through a 100-μm mesh filter into four 15-cm culture dishes.
(y) Incubate the dishes for 1 h in the CO_2 incubator. During this time, fibroblasts and other noncardiac myocytes adhere, whereas cardiac myocytes remain floating.
(z) Transfer nonadherent cells to a 50-ml tube, sediment by centrifugation, resuspend the pellet in fresh complete medium, and count cells.
(aa) Adjust the cell concentration to 6.4×10^6 cells/ml. Cell yield per animal is generally $2–3 \times 10^6$ viable cells/heart as judged by trypan blue exclusion.

3.2. Engineered Heart Tissue Reconstitution Mixture

A typical reconstitution mixture for 4 EHTs is shown in following Protocol and is prepared on ice in 10-ml tubes.

Protocol 11.2. Preparation of Reconstituted Rat Heart Tissue

Reagents and Materials

Sterile

- ❑ Collagen type I (rat tail)
- ❑ Concentrated DMEM, 2× (See Section 2.6)
- ❑ NaOH

- ❑ Basement membrane proteins: Matrigel® or Harbor ECM
- ❑ Freshly isolated cell suspension
- ❑ Plastic tubes, 10 ml

Non-sterile

- ❑ Ice bath

Protocol

Prepare the following typical reconstitution mixture for 4 EHTs on ice:

	Concentration	Volume	Total
Collagen type I (rat tail)	4.2 mg/ml	847 μl	3.56 mg
Concentrated DMEM	2×	847 μl	
NaOH	0.1 M	184 μl	
Basement membrane proteins (Matrigel®)	As purchased	400 μl	
Freshly isolated cell suspension	6.4×10^6/ml	1722 μl	11×10^6
Total volume		4000 μl	

The volumes are calculated for a total volume of 3.6 ml (900 μl per EHT) plus 10%. Volumes of collagen I and 2× concentrated culture medium must be adapted according to the actual collagen I concentration in the batch. The volume of NaOH is ignored in the calculation of the volume of concentrated medium.

The optimal reconstitution mix has been the result of extensive testing of the effects of cell number, both in the original lattice model [Zimmermann et al., 2000] and in the ring model [Eschenhagen et al., 2002]. As outlined above (See Section 1), an increase in cell number up to 2.5×10^6 cells/EHT in the lattice model improved contractile force, but a further increase sharply deteriorated it. In contrast, cell number could be increased up to 10×10^6 cells/EHT in the ring model without worsening. A cell density $>2.5 \times 10^6$/EHT did not improve function, but led to faster condensation of the cell-matrix mix. Collagen I was found optimal at 0.5–0.8 mg/EHT. A lower collagen content resulted in unstable and only weakly contracting EHTs, whereas a higher collagen content yielded EHTs that were rigid and developed less active force. A collagen content of 0.8 mg/EHT was chosen for mechanical stability, easier handling, and optimal contractile function.

Matrigel was essential for any tissue development in rat EHTs and improved force at concentrations between 5% and 15% (v/v). We chose 10% (v/v) in our standard EHT construction mixture as a compromise between function and costs. Chick embryo extract could be omitted on day 7 without significant effect on force development but was essential during the initial culture period [Zimmermann et al., 2003]. In contrast, even small reductions in horse serum concentration (to 3%) starting on day 7, 8, or 9 of culture prevented condensation of the cell-matrix

mix and almost completely abolished contractile function when measured at day 14 [Eschenhagen et al., 2002].

3.3. Cultivation of Engineered Heart Tissue

Circular casting molds (diameter: 16 mm, depth: 5 mm) are prepared in glass culture dishes (diameter: 50 mm).

Protocol 11.3. Preparing Casts and Culturing Engineered Rat Heart Tissue

Reagents and Materials

Sterile

- ❑ Reconstitution mixture, ice-cold (See Protocol 11.2)
- ❑ Complete medium (See Section 2.1)
- ❑ Petri dishes, 3.5 and 5 cm

Non-sterile

- ❑ Silicone tubes (length: 10 mm, diameter: 2 mm)
- ❑ Teflon disks (diameter: 16 mm, depth: 5 mm, central hole diameter: 2 mm)
- ❑ Teflon cylinders (diameter: 8 mm, height: 10 mm)
- ❑ Liquid silicone glue
- ❑ Mechanical stretching device (See Fig. 11.4c, Color Plate 6B)

Protocol

(a) Glue two silicone tubes (length: 10 mm, diameter: 2 mm) to the surface of the 5-cm Petri dish to hold reversible Teflon disks (diameter: 16 mm, depth: 5 mm, central hole diameter: 2 mm) serving as spacers while liquid silicone glue is poured into the culture dish. Teflon spacers can be removed after hardening of the silicone glue to yield circular casting molds (See Fig. 11.4a, Color Plate 6B).

(b) Leave casting molds for at least 2 weeks to ensure that silicone has thoroughly hardened and solvents have evaporated.

(c) Wash molds and boil in distilled water before use. Subsequently, sterilize by autoclaving. Casting molds can be reused infinitely.

(d) Before EHT casting, place removable Teflon cylinders (diameter: 8 mm) over each silicone tubing to yield circular wells (750 mm^3). The size of a casting mold is sufficient to hold the viscous reconstitution mixture (900 μl) in place.

(e) Pipette the ice-cold reconstitution mixture into the mold at room temperature.

(f) Transfer the molds to the 37 °C incubator for 1 hour.

(g) Remove from the incubator, add 6 ml culture medium, and return to the incubator.

(h) Culture EHTs in the casting mold for 7 days at 37 °C, in a 5% CO_2-95% air, humidified atmosphere.

(i) Change the medium after the initial overnight culture and then every other day.

(j) After 7 days, transfer the ring-shaped EHTs to the mechanical stretching device (See Fig. 11.4c, Color Plate 6B) and subject to phasic horizontal stretch at 2 Hz and a lateral strain of 10% from the original EHT length (8- to 8.8-mm internal diameter) in 3.5-cm Petri dishes with 6 ml culture medium for 5–7 days.
(k) Change medium every day during stretching.

Protocol 11.4. Force Measurement in Engineered Heart Tissue

Reagents and Materials

Sterile

- ❑ Precast and cultured EHTs

Non-sterile

- ❑ Modified Tyrode's solution (See Section 2.3) with 0.4 mM Ca^{2+}
- ❑ Organ baths, thermostatically controlled at 37 °C
- ❑ Force transducer

Protocol

(a) Suspend EHTs individually at slack length in 30-ml organ baths at 37 °C fixed between a lower fixed holder and a stainless steel wire connected to the force transducer (See Fig. 11.4d, Color Plate 6B). Tyrode's solution (equilibrated to a pH of 7.4 by continuous bubbling (approximately 30 min) with 95% O_2 – 5% CO_2) with 0.4 mM calcium is used for the initial equilibration and adjustment of EHTs.
(b) After 15 min without pulsing, continue equilibration under electrical stimulation with rectangular pulses (2 Hz, 5 ms, 80–100 mA) until force development and contraction kinetics of EHT reach a steady state (approximately additional 15 min).
    i) Subsequently, preload is adjusted from approximately 0.05–0.1 mN (at slack length) to L_{max}, i.e., the length at which EHTs developed maximal active force.
    ii) Resting tension at L_{max} normally amounts to 0.2–0.3 mN.
    iii) Equilibration and preload adjustment takes about 60 min.
(c) After a change of the Tyrode's solution, measure inotropic (change of force of contraction) and lusitropic (change of contraction kinetics/times) responses to cumulative concentrations of calcium (0.2–2.8 mM) and isoprenaline (0.1–1000 nM) at 0.2 mM baseline calcium concentrations [Zimmermann et al., 2002a]. Twitch tension (TT; systolic force), resting tension (RT; diastolic force), contraction duration (T1: time from 10% to peak force development), and relaxation duration (T2: time from peak contraction to 90% relaxation) are evaluated by BMON software (Ingenieurbüro Jäckel, Hanau, Germany).

4. GENE TRANSFER IN ENGINEERED HEART TISSUE

The most efficient way to transfect cardiac myocytes (and other cell types in EHT) is adenoviral gene transfer. We generally purify our virus by cesium chloride density centrifugation and dialysis and store virus stock in 30% glycerol at $-20\,^{\circ}C$. Virus titration is performed in neonatal rat cardiac myocytes by serial dilutions. The transfection rate of 100% would correspond to 2×10^6 biologically active virus (bav) for 2×10^6 cells. This titer is used to calculate the multiplicity of infection (MOI). A MOI of 1 is, by our definition, sufficient to yield 100% transfection of cultured neonatal rat cardiac myocytes.

In EHT we use an MOI of 50 to get similarly high transfection rates (1.25×10^8 bav/EHT). The necessity to utilize higher virus titers than in 2D cultures of neonatal rat cardiac myocytes could result from the advanced maturation of cardiac myocytes in EHTs. Accordingly, high titers (MOI of 100–10,000) must be utilized to reach comparable transfection rates in adult cardiac myocytes [El-Armouche et al., 2003]. This phenomenon might be attributed to the downregulation of the common coxsackievirus and adenovirus receptor (CAR) during cardiac myocyte differentiation and aging [Communal et al., 2003; Fechner et al., 2003].

Generally, we perform adenovirus infections on EHT culture day 10 under serum-free conditions by directly pipetting adenovirus into the culture medium (5 ml) in which the EHT is (or 2 EHTs are) maintained (See Fig. 11.4c, Color Plate 6B). An aliquot of a virus dilution in serum-free DMEM is pipetted directly into the culture dish containing one or two stretched EHTs (See Fig. 11.4b, Color Plate 6B). After 1 hour, 5 ml of complete medium is added. Functional responses are generally evaluated 48 h after infection. If a virus is used that codes for green fluorescent protein, transfection efficiency can be monitored in the living EHT (Fig. 11.5, See Color Plate 6C) [El-Armouche et al., 2003].

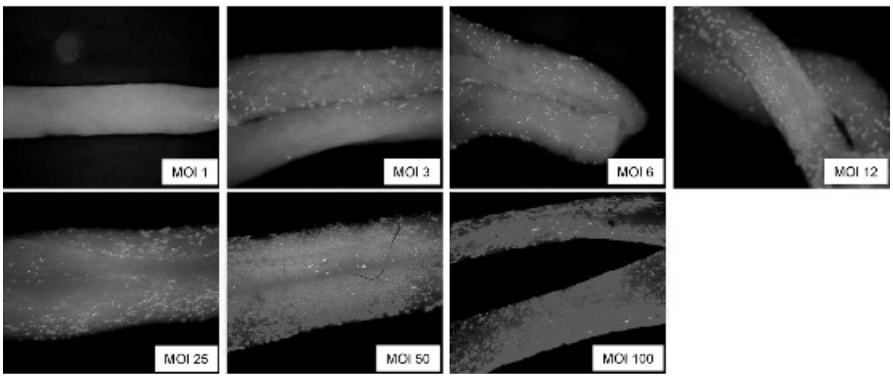

Figure 11.5. Adenoviral gene transfer in EHT. EHTs were infected with increasing virus concentrations/cell of AdPPI-1/GFP. Transfection of cells was visualized by fluorescence of the coexpressed GFP 48 h after infection. Note increasing numbers of cells showing GFP fluorescence throughout EHTs. From El-Armouche et al. [2003]. (See Color Plate 6C.)

5. HISTOLOGIC PROCEDURES IN ENGINEERED HEART TISSUE

Protocol 11.5. Conventional Histology of Engineered Heart Tissue

Reagents and Materials

Non-sterile

- ❑ Fixative (See Section 2.7)
- ❑ PBS
- ❑ Agar, 2%
- ❑ Isopropanol in graded concentrations
- ❑ Paraffin-isopropanol 1:1
- ❑ Melted paraffin wax
- ❑ Embedding oven
- ❑ Microtome
- ❑ Stains: hematoxylin and eosin (H&E), Masson Goldner trichrome, or Sirius red

Protocol

(a) For paraffin embedding fix (See Section 2.7) EHTs overnight at 4 °C.
(b) Wash and soak overnight in PBS.
(c) Embed EHTs in 2% agar blocks.
(d) Dehydrate in graded concentrations of isopropanol, paraffin-isopropanol, and embed in paraffin according to standard procedures.
(e) Stain horizontal and cross sections (4 μm) of EHTs with hematoxylin and eosin (H&E), Masson Goldner trichrome, or Sirius red to evaluate cell-matrix composition of EHTs.

For confocal laser scanning microscopy and immunofluoresence studies EHTs are fixed and embedded in agar as described above or used as whole mount samples after fixation. We found that, in contrast to cultured cells, EHTs tend to create more nonspecific background staining. This is most likely due to a high nonspecific binding of most antibodies to highly charged collagen. Moreover, thick sections or whole mounts that are preferentially used to get a 3D image of the EHT structure add the problem of antibody diffusion. The experimental procedures explained in Protocol 11.6 have been adapted accordingly.

Protocol 11.6. Confocal Immunofluorescence of Engineered Heart Tissue

Reagents and Materials

Non-sterile

- ❑ Supplemented Tris-buffered saline (STBS) (See Section 2.8)
- ❑ Primary and secondary antibodies (See Table 11.1)
- ❑ Vibratome slicer
- ❑ Confocal microscope

Protocol

(a) Prepare sections (100 μm) of agar-embedded EHTs with a vibratome slicer.
(b) Block nonspecific binding in vibratome and whole mount samples and permeabilize by keeping at 4 °C overnight in STBS.
(c) After two washes in STBS incubate sections/whole mounts with the primary antibodies at 4 °C for 48 h. Table 11.1 gives antibodies, dilutions and sources for α-sarcomeric actinin, α-sarcomeric actin, myomesin, α-smooth muscle actin, prolyl-4-hydroxylase, CD31, and the macrophage marker ED2.
(d) After an overnight wash in STBS incubate sections/whole mounts with secondary antibodies at room temperature for 3 h.
(e) Perform confocal imaging, e.g., with a Zeiss LSM 5 Pascal system using a Zeiss Axiovert microscope.

Protocol 11.7. Transmission Electron Microscopy of Engineered Heart Tissue

Reagents and Materials

Non-sterile

- ❑ Glutaraldehyde, 2.5% (See Section 2.9)
- ❑ Osmium tetroxide-PBS, 1:1
- ❑ PBS
- ❑ Graded ethanol concentrations
- ❑ Acetone
- ❑ Uranyl acetate
- ❑ Lead citrate
- ❑ Epon
- ❑ Ultramicrotome
- ❑ Electron microscope

Protocol

(a) For transmission electron microscopy, fix EHTs in 2.5% glutaraldehyde (See Section 2.9) overnight at 4 °C.
(b) After an overnight wash in PBS, postfix EHTs in osmium tetroxide-PBS, 1:1, for 2 h at room temperature.
(c) After an overnight wash in PBS at 4 °C, dehydrate samples in graded ethanol and acetone, infiltrate with epon/acetone, and embed in epon according to standard protocols.
(d) Stain semithin sections (1 μm) with toluidine blue.
(e) For TEM, cut ultrathin sections (50 nm) and contrast with uranyl acetate and lead citrate.
(f) Examine sections with, e.g., a Zeiss Leo 906 EM system.

6. REPRESENTATIVE TISSUE CULTURE STUDY

A recent study characterized EHTs from neonatal rat cardiac myocytes [Zimmermann et al., 2002a]. The main results of this study are presented here. Methods have been presented in detail in Section 5.

6.1. Casting and Culture of Circular EHTs

Circular EHTs can be cast easily in large series. On average we reconstituted 30 EHTs from 30 neonatal rat hearts per week. During culture the EHTs condensed around the removable central Teflon cylinder within the casting molds (See Fig. 11.4b, Color Plate 6B). First contractions of single cells were noted after 24 h, synchronous contractions of cell clusters started at day 2. The size of beating clusters increased until the entire EHT beat synchronously (~1 Hz, day 4–5). Over time, contraction became more regular, more vigorous, and faster (~2 Hz). Physical stability to allow manual handling and mechanical stretch without inflicting damage to the EHT structure was reached after 6–7 days in culture. Vigorous spontaneous contractions of EHTs were noted when the stretch device was turned off and after transfer of EHTs into a culture dish [video sequence at http://circres.ahajournals.org/cgi/content/full/90/2/223/DC1]. At this stage EHTs weighed 29.2 ± 1.4 mg ($n = 12$) and had a diameter of 833 ± 17 μm ($n = 16$).

6.2. Histology

In planar EHT lattices, called cardiomyocyte-populated matrices (CMPMs; [Eschenhagen et al., 1997]), cardiac myocytes were mainly concentrated at the lateral free edges. In contrast, serial sections of paraffin-embedded circular EHTs ($n = 7$) did not reveal a spatial preference of cell distribution. Complexes of multicellular aggregates and longitudinally oriented cell bundles mainly consisting of cardiac myocytes (Fig. 11.6a, See Color Plate 6D) were found throughout circular EHTs. The width of these muscle bundles ranged from 30 to 100 μm. For comparison, paraffin sections of native heart tissue from newborn, neonatal, and adult rats (300 g) were investigated (Fig. 11.6b–d, See Color Plate 6D). In the adult myocardium, compared to the immature tissues, myocytes were larger in width and length, were more intensely stained with eosin, and exhibited clear cross-striation, indicating a higher content of myofilaments. Density of myocyte and nonmyocyte nuclei was approximately threefold lower in the adult tissue, and myocyte nuclei were elongated (length to width 5:1) in contrast to round or oval nuclei in the immature tissue. Surprisingly, histologic features of myocytes forming EHTs resembled those of myocytes within native differentiated myocardium. The intensity of eosin staining was higher than in the immature tissues, cross-striation was visible, albeit to a lesser degree than in the adult tissue, and nuclei had a length-width ratio of 5–6. Other differences from the adult tissue included smaller size of cardiac myocytes and their nuclei and a less compact overall structure.

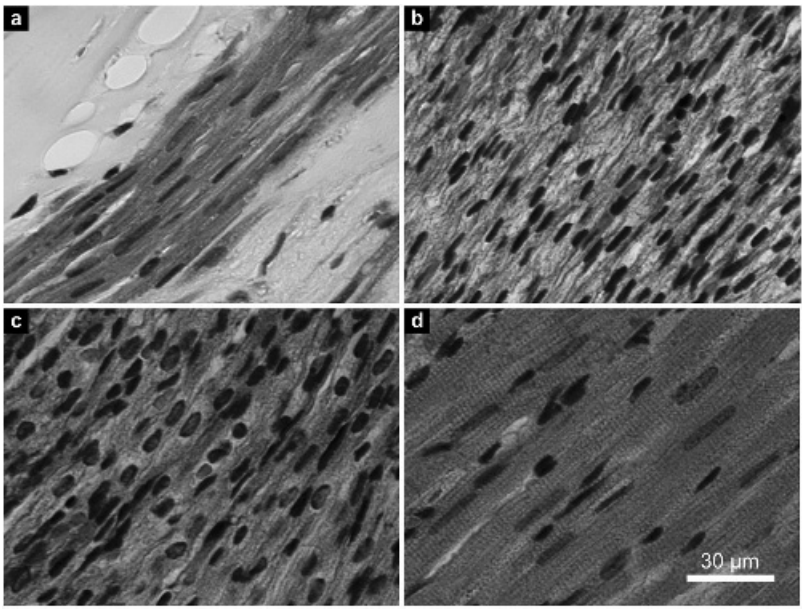

Figure 11.6. Morphology of EHTs and native myocardium. H&E staining of paraffin sections of EHT (a) and native myocardium from newborn (0 dpp; b), 6-day-old (c), and adult (300 g; d) rats. All sections were prepared, fixed, and stained in parallel to allow direct comparison of eosin staining. Note that cardiac muscle bundles in EHTs, even though derived from neonatal rat hearts (0–3 dpp), resemble cardiac morphology in the adult heart more closely than in neonatal myocardium. From Zimmermann et al. [2002a] (See Color Plate 6D).

6.3. Immunoconfocal Characterization of EHTs

To analyze the overall composition and spatial distribution of cell species within EHTs, vibratome sections were immunolabeled to identify cardiac myocytes (α-sarcomeric actin), smooth muscle cells (α-smooth muscle actin), fibroblasts (prolyl-4-hydroxylase), and macrophages (ED2 antigen). Cardiac myocytes (Fig. 11.7a, See Color Plate 6E) constituted the majority of the phalloidin-tetramethylrhodamine isothiocyanate (TRITC)-positive cellular network (Fig. 11.7b,e,h,k, See Color Plate 6E). Smooth muscle cells, positive for α-smooth muscle actin, lined the outer surface of EHTs (Fig. 11.7d, See Color Plate 6E). Some α-smooth muscle actin-positive cells within EHTs may represent smooth muscle cells or immature cardiac myocytes. Fibroblasts and macrophages were scattered throughout EHTs (Fig. 11.7g–l, See Color Plate 6E).

Whole-mount preparations of EHTs were stained with phalloidin-TRITC and examined by confocal laser scanning microscopy (CLSM) (Fig. 11.8, See Color Plate 6F). This technique revealed cell strands forming a network of intensively interconnected cell bundles throughout the entire EHT (Fig. 11.8a, See Color Plate 6F), which condensed to solid muscle bundles at variable positions inside the EHT as depicted in Fig. 11.6a and Color Plate 6D. High-power CLSM demonstrated that the majority of cell bundles were composed of cardiac myocytes with a high

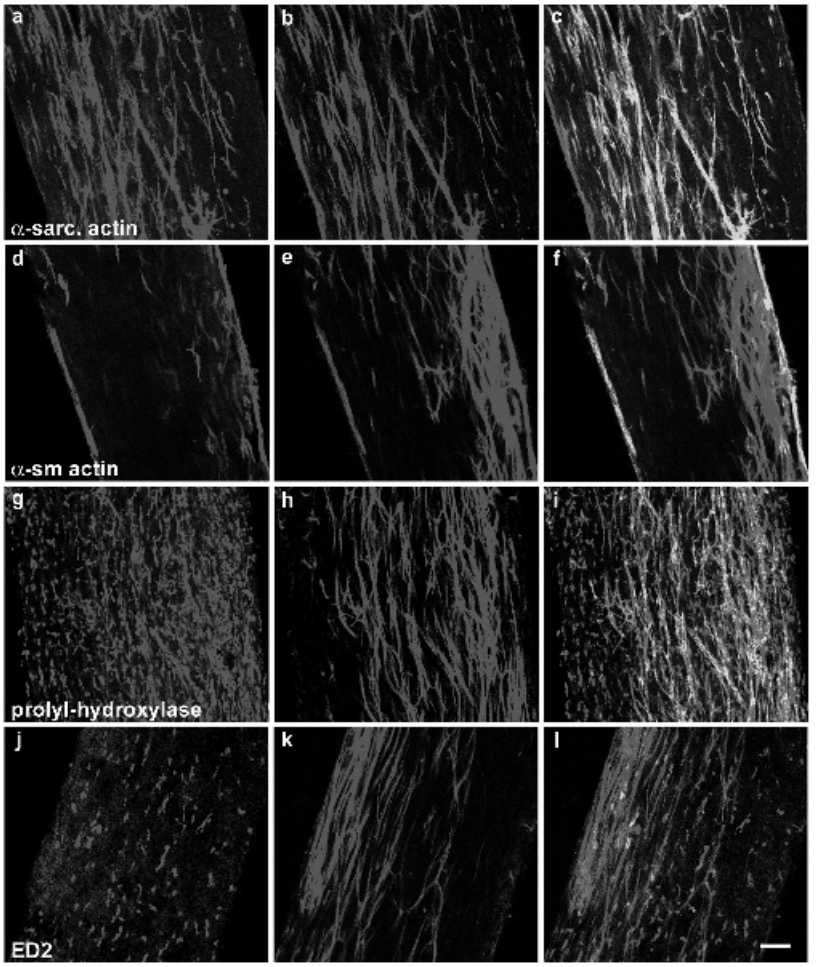

Figure 11.7. Immunolabeling of distinct cell species within EHT. Cellular composition and localization was investigated by immunolabeling (green) of cardiac myocytes (α-sarcomeric actin; a), smooth muscle cells (α-smooth muscle actin; d), fibroblasts (prolyl-4-hydroxylase; g), and macrophages (ED2-antigen; j). Actin filaments were labeled with phalloidin-TRITC (red; b,e,h,k). Superposition of images (c,f,i,l) yields a yellow signal where double fluorescent labeling was achieved. Bar: 100 μm. From Zimmermann et al. [2002a]. (See Color Plate 6E.)

degree of sarcomeric organization (Fig. 11.8b,c, See Color Plate 6F). At high magnification, capillary structures positive for CD31 (platelet endothelial cell adhesion molecule, PECAM) were noted (Fig. 11.8d, See Color Plate 6F).

6.4. Ultrastructural Characterization of EHTs

Ultrastructural hallmarks of cardiac myocyte differentiation are M-band formation, development of T-tubules with dyads/triads, specialized cell-cell junctions, and the reestablishment of an extracellular basement membrane [Anversa et al., 1981; Bishop et al., 1990; Katz, 1992]. Most, but not all, of these features were

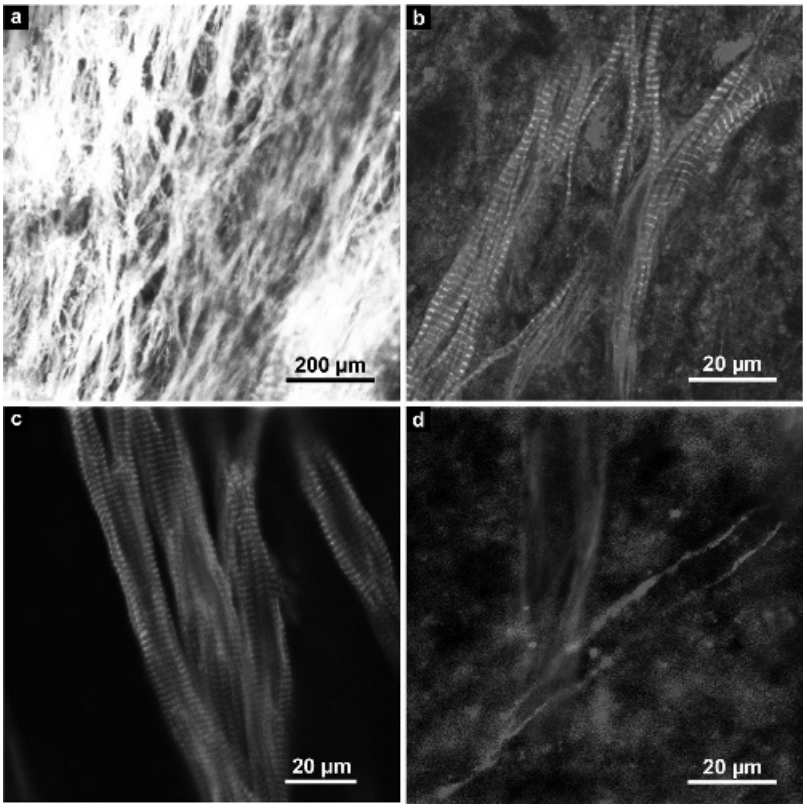

Figure 11.8. High-power CLSM of EHT. a) Extended focus imaging of a whole mount EHT after staining with phalloidin-TRITC. EHTs consist of a dense network of mainly longitudinally oriented cell bundles. b,c) Confocal images (optical slice: 1–2 µm) of vibratome sections (100 µm) of EHTs. Actin (red), myomesin (green; b), actinin (green; c). Note that cell bundles mainly consist of longitudinally oriented cardiac myocytes with sarcomeres in registry. d) Detection of CD31-positive capillary structures in vibratome sections (actin: red; CD31: green). From Zimmermann et al. [2002a] (See Color Plate 6F).

present in the majority of cells (Figs. 11.9, 11.10). Cardiac myocytes within EHTs displayed a predominant orientation of sarcomeres in registry along the longitudinal cell axis (Fig. 11.9a). Cross sections of EHT revealed that most cardiac myocytes were densely packed with myofibrils and mitochondria (Fig. 11.9b).

Morphometric evaluation of 20 longitudinally oriented, mononucleated cardiac myocytes from four EHTs revealed volume fractions as follows: myofibrils ($44.7 \pm 1.9\%$), mitochondria ($23.9 \pm 1.2\%$), nuclei ($8.9 \pm 0.9\%$). The rest ($22.5 \pm 1.8\%$) was occupied by sarcoplasmic reticulum (SR), cytoplasm, and undefined structures. Sarcomeres were composed of Z-, I-, A-, and H-bands in most investigated cells. Immature M-bands were noted frequently, but not in all sarcomeres. If present (Fig. 11.10a), they were clearly less developed than in adult myocytes, indicating that cardiac myocytes in EHTs exhibit a high, but not terminal, degree of differentiation. T-tubules were observed at the Z-band level (Fig. 11.10b-d) and often

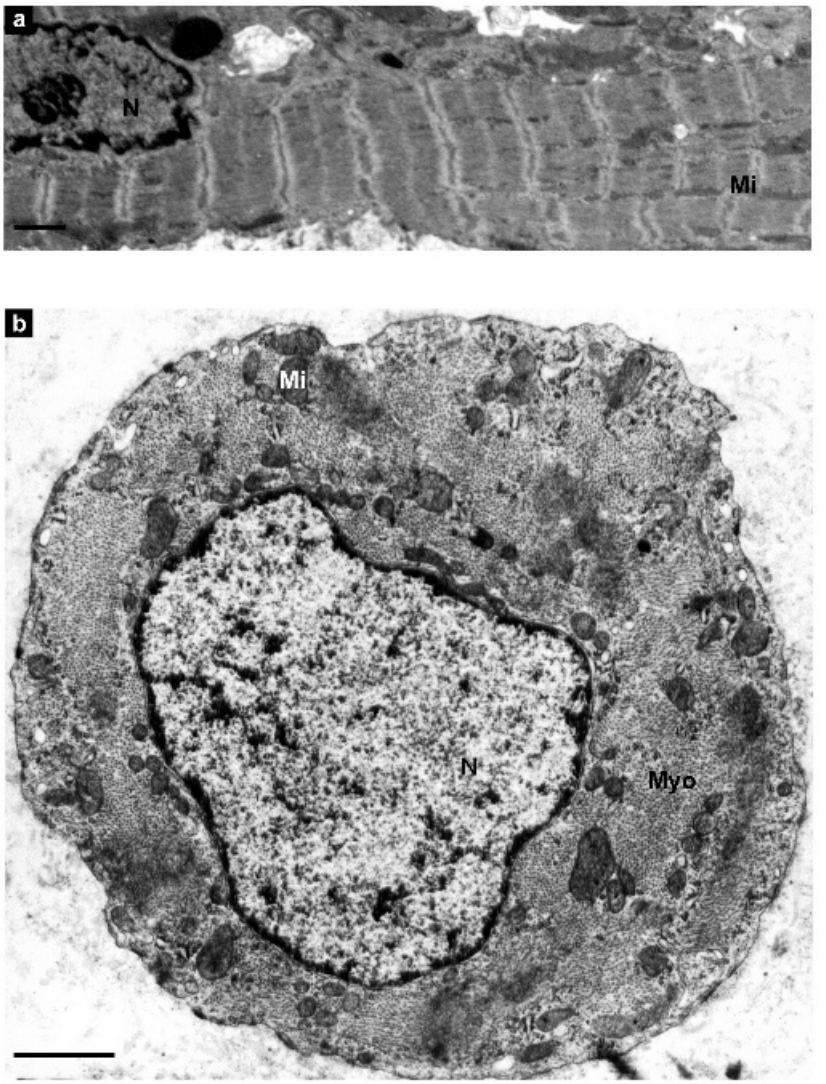

Figure 11.9. TEM of cardiac myocytes within EHT. a) Cardiac myocytes are filled with well-aligned sarcomeres. Note orientation of sarcomeres in registry along the longitudinal axis of the cell. Mitochondria (Mi) are mainly located in the intermyofibrillar space or the perinuclear region (not shown). b) A cross section demonstrates the density of myofibrils (Myo) intermingled with mitochondria in cardiac myocytes reconstituted to EHT. Note the centrally located nucleus (N). Bars: 1 μm. From Zimmermann et al. [2002a].

formed dyads with the SR (Fig. 11.10c, d). Specialized cell-cell junctions responsible for mechanical and electrical coupling of cardiac myocytes (adherens junctions, desmosomes, gap junctions) were found throughout EHTs (Fig. 11.10d, e). Cardiac myocytes often formed a well-developed basement membrane as an additional indication of cardiac myocyte integrity (Fig. 11.10f). Atrial secretory granules characteristic for atrial or undifferentiated ventricular myocytes were absent.

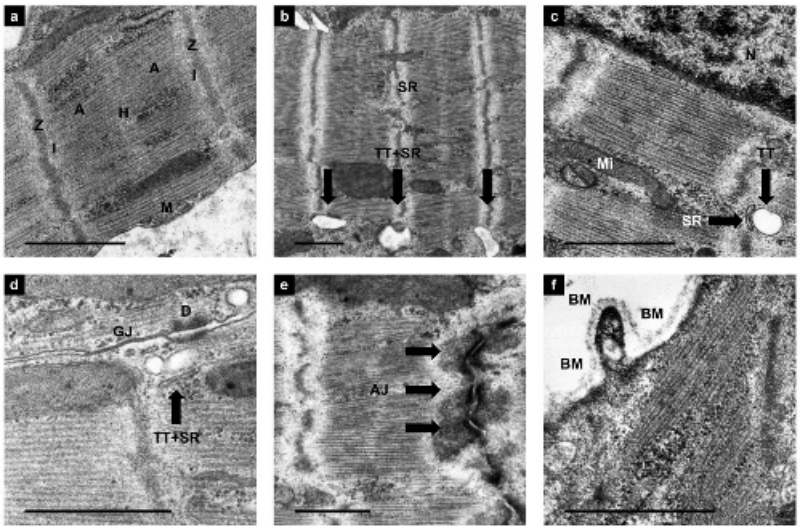

Figure 11.10. TEM of sarcomeric structures, cell-cell junctions, and basal membrane of cardiac myocytes in EHT. a) Formation of (immature) M-bands was noted in some but not all cardiac myocytes, while Z-, I-, A-, and H-bands were clearly distinguishable in most cardiac myocytes in EHT. b–d) T-tubules (TT) of various diameters. Dyad formation with sarcoplasmic reticulum (SR) was found frequently, especially at the Z-band level. d,e) Gap junctions (GJ), desmosomes (D), and adherens junctions (AJ) interconnect 3D reconstituted cardiac myocytes. f) Well-developed basement membrane (BM) around reconstituted cardiac myocytes. Bars: 1 μm. From Zimmermann et al. [2002a].

TEM provided additional evidence that EHTs are reconstituted of various cell species apart from cardiac myocytes resembling an organoid cardiac tissue construct (Fig. 11.11). These cells did not populate EHTs in a random fashion, but formed distinct structures. The outer surface of EHTs was lined with multiple cell layers consisting mainly of nonmyocytes (fibroblasts, smooth muscle cells, endothelial cells, macrophages; Fig. 11.11a). Fibroblasts, sometimes clearly demonstrating secretory activity, were found throughout EHTs (Fig. 11.11b, also Fig. 11.7g–i, See Color Plate 6E). Endothelial cells formed characteristic capillary structures that corresponded to CD31-positive cells observed by CLSM (Fig. 11.11c and Fig. 11.7d, See Color Plate 6E). Cell debris was frequently sequestrated by macrophages (Fig. 11.11d).

6.5. Contractile Properties of Circular EHTs

Contractile force and twitch kinetics of electrically stimulated EHTs were investigated under isometric conditions. At L_{max}, twitch tension (TT) amounted to 0.36 ± 0.06 mN at a resting tension (RT) of 0.27 ± 0.03 mN. Contraction and relaxation time (T1 and T2) were 83 ± 2 ms and 154 ± 9 ms, respectively. An increase in extracellular calcium enhanced TT from 0.34 ± 0.06 to 0.75 ± 0.11 mN, with a maximal inotropic response at 1.6 mM (Fig. 11.12a), RT and twitch kinetics remained unchanged. β-Adrenergic stimulation induced a maximal increase of TT

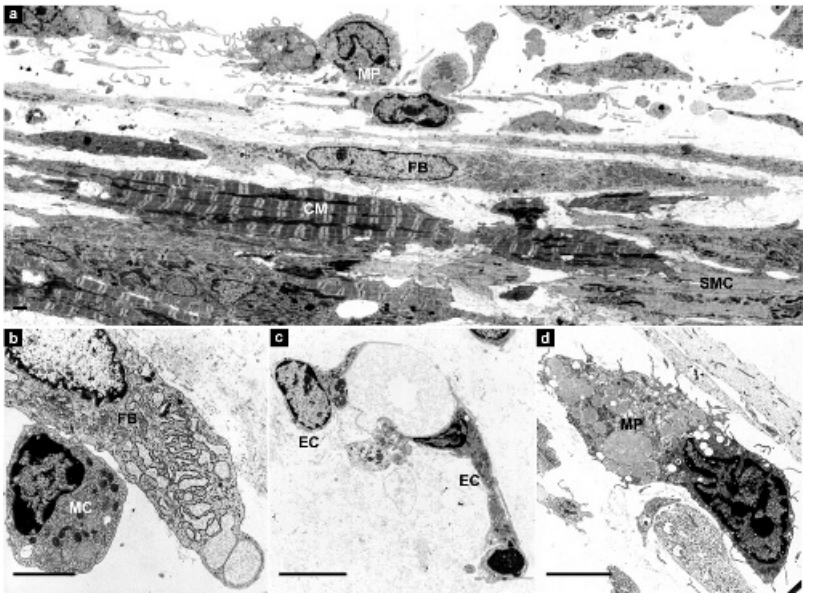

Figure 11.11. TEM of various cell types found to populate EHT. a) Macrophages (MP), fibroblasts (FB), and other cells with a low degree of differentiation lined the outer surface of EHTs. Underneath, a cell layer mainly consisting of cardiac myocytes (CM) and smooth muscle cells (SMC) can be observed. b) Fibroblasts (FB) with and without signs of secretory activities were found throughout EHT. c) Endothelial cells (EC) were noted to form capillary structures within EHT. d) Cells of leukocytotic origin like macrophages and other mononucleated cells (MC; b) were found mainly at the EHT surface but also within EHT. Bars: 1 μm. From Zimmermann et al. [2002a].

from 0.28 ± 0.06 to 0.69 ± 0.09 mN at 1 μmol/l isoprenaline (Fig. 11.12b). Additionally, isoprenaline shortened T1 from 86 ± 4 to 56 ± 2 ms and T2 from 144 ± 8 to 83 ± 3 ms and reduced RT from 0.15 ± 0.02 to 0.05 ± 0.02 mN (Fig. 11.12c,d). The decrease in RT may be mediated by smooth muscle cells that line the surface of EHTs (Fig. 11.12d–f).

6.6. Action Potentials

After equilibration in Tyrode's solution, EHT preparations generated only very infrequent spontaneous action potentials. Electrical stimulation at 1 Hz elicited regular action potentials with fast upstroke velocity (dV/dt_{max} : 66 ± 8 V/s), amplitude of 109 ± 2 mV, and a prominent plateau phase with action potential duration at 20%, 50%, and 90% repolarization of 52 ± 2, 87 ± 4, and 148 ± 3 ms, respectively (Fig. 11.13). In all six experiments resting potential (-73 ± 2 mV) was stable during electrical diastole.

7. DISCUSSION

This chapter describes a method to engineer a 3-dimensional cardiac tissue-like construct in vitro (EHT). Compared to planar lattices, ring-shaped EHTs exhibit

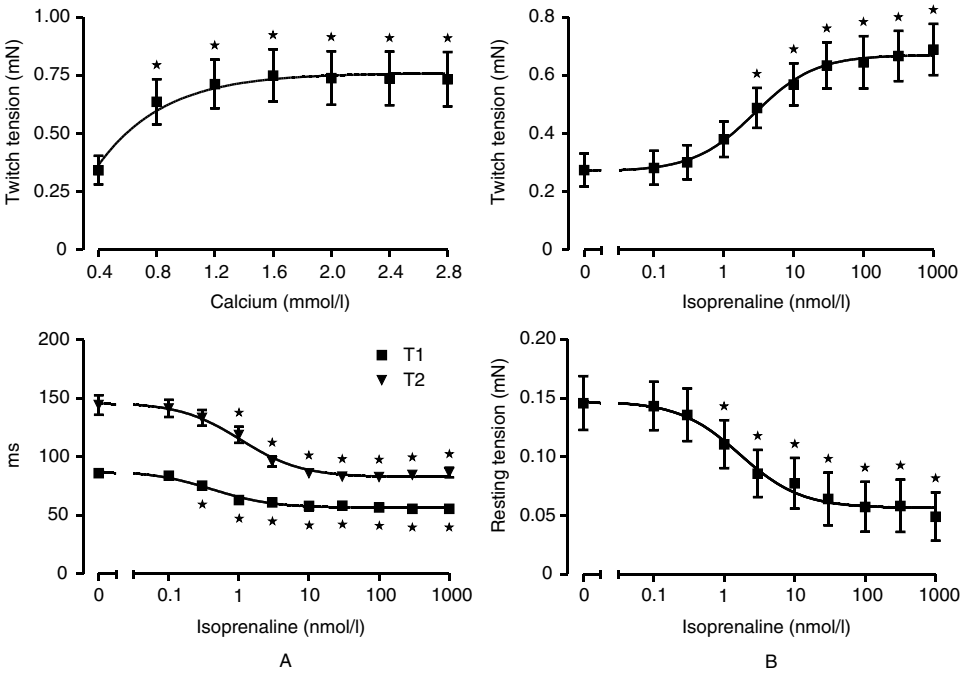

Figure 11.12. Contractile response to calcium and isoprenaline. a) The effect of calcium ($n = 15$, 7 independent cell preparations) was evaluated by cumulatively increasing calcium from 0.4 to 2.8 mM (calculated EC_{50}: 0.46 ± 0.06 mM). b,c) The effect of isoprenaline ($n = 12$, 6 independent cell preparations) was tested at 0.4 mM calcium by cumulatively increasing isoprenaline from 0.1 to 1000 nmol/l (EC_{50}: 2.8 ± 0.6 nmol/l). d) Additionally, isoprenaline lowered RT. *Significant differences ($P < 0.05$; repeated-measures ANOVA with post hoc Bonferroni test) to force at 0.4 mM calcium (a) or predrug value (b–d). From Zimmermann et al. [2002a].

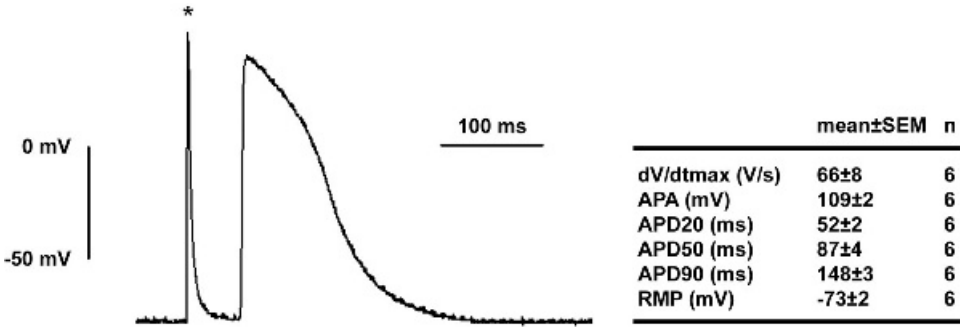

	mean±SEM	n
dV/dtmax (V/s)	66±8	6
APA (mV)	109±2	6
APD20 (ms)	52±2	6
APD50 (ms)	87±4	6
APD90 (ms)	148±3	6
RMP (mV)	-73±2	6

Figure 11.13. Action potential recording from EHT. Original intracellular recording of a representative EHT action potential at 36 °C. *Stimulus artifact. dV/dt_{max}: maximum upstroke velocity; APA: action potential amplitude; APD: action potential duration at 20%, 50%, and 90% repolarization; RMP: resting membrane potential. From Zimmermann et al. [2002a].

a better cardiac tissue-matrix ratio (area fraction occupied by cellular material as compared to pure matrix), improved contractile function, and a high degree of cardiac myocyte differentiation. Action potential recordings revealed electrophysiological properties typical for cardiac tissue. The culture as 3D rings is simple, does not require special equipment, and can therefore be performed in any cell culture laboratory. Importantly, the circular culture format allows for future miniaturization and automation.

7.1. In Vitro Applications

The main advantage of EHTs in our view is that cardiac myocytes in EHTs resemble cardiac myocytes in the intact heart more closely than standard 2D culture systems. This interpretation is supported by the following findings.

1. The cells form a 3D network of intensely interconnected, strictly longitudinally oriented, electrically and mechanically coupled bundles that resemble loose cardiac tissue.
2. The cells are apparently exposed to homogeneous load. The latter feature has not been proven directly (and it would be difficult to do so), but both the fact that the cellular network in EHTs was strictly longitudinally oriented and the geometry of a ring argue for a homogeneous load. As a consequence, tissue formation was much more homogeneous in circular EHTs than in the previously used planar lattices [Eschenhagen et al., 1997; Zimmermann et al., 2000; Fink et al., 2000].
3. In accordance with the organized tissuelike morphology, circular EHTs exhibited a tissuelike ratio of twitch tension to resting tension of 1.33, 3.29, and 14.02 under basal, maximal calcium, and maximal isoprenaline concentrations, respectively. The basal values are in line with similar ratios in intact trabeculae or papillary muscles from humans and rats studied under the same conditions [Weil et al., 1998; Holubarsch et al., 1996; Mende et al., 1992]. This indicates that in circular EHTs the matrix contributes significantly less to mechanical properties than in the planar lattices, where we have described a ratio of twitch tension to resting tension of 0.2–0.3 [Eschenhagen et al., 1997; Zimmermann et al., 2000; Fink et al., 2000].
4. The positive inotropic response to isoprenaline amounted to more than 100% of basal twitch tension in circular EHTs compared to only about 15–30% in the planar lattices. This better resembles the magnitude of the isoprenaline effect in intact rat preparations, where we have reported an isoprenaline-induced increase in twitch tension by 114–145% (EC_{50}: 110 nM) under the same conditions, albeit at a calcium concentration of 1.8 mM [Mende et al., 1992]. The reason for the high sensitivity to isoprenaline in EHTs (EC_{50}: 2.8 nM) remains unclear and parallels the previously observed leftward shift of the calcium response curve in the EHT model [EC_{50}: 0.46 mM vs. 3.1 mM in adult rat papillary muscles; own unpublished data].

5. EHTs are suitable for electrophysiological investigations usually performed on isolated multicellular cardiac preparations, for example, papillary muscles. Six intracellular recordings on EHTs revealed stable resting membrane potentials and action potentials similar to those found in ventricular myocytes from young rats [Kilborn and Fedida, 1990].

6. Cardiac myocytes in EHTs exhibited several morphological features of terminal differentiation [Anversa et al., 1981; Bishop et al., 1990; Katz, 1992]: (a) Densely packed and highly organized sarcomeres; (b) an adult cardiac myocyte-like volume ratio of myofilaments-mitochondria-nucleus of 45:24:9 with the remaining 23% consisting mainly of SR and cytosol, which compares to published data on adult cardiac myocytes of 47:36:2 and 3.5% SR, 11.5% cytosol [Katz, 1992]; (c) all types of normal intercellular connective structures such as adherens junctions, desmosomes, and gap junctions; (d) T-tubules, SR vesicles and T-tubule-SR junctions in form of dyads; and (e) a well-developed basement membrane surrounding cardiac myocytes. It is important to note that some of the features observed in EHTs, especially the T-tubule-SR junctions, were found to be absent in the newborn rat heart [Bishop et al., 1990] and in monolayer cultures of cardiac myocytes [Kostin et al., 1998]. In addition, during the cell isolation procedure, cardiac myocytes lose or disassemble much of their myofilament equipment and appear as rounded cells at the time they are put into the medium-collagen-Matrigel mix. It is remarkable, therefore, that during 14 days of in vitro cultivation they surpass the differentiation state of their source tissue.

7. The electron microscopic investigation also revealed that cardiac cells form not only a myocyte network, but a complex heartlike structure with multiple layers of nonmyocytes at the surface and endothelial cells forming primitive capillaries inside EHTs. Fibroblasts and macrophages were seen throughout the EHTs, suggesting that EHTs represent spontaneously forming cardiac "organoids." The conditions controlling this process or its functional consequences have not been studied here, but the findings may open the possibility of using this system as a model for in vitro cardiac development.

8. Finally, for in vitro applications, technical aspects are also important. The ring system requires only simple casting forms that can be used infinitely and allow the routine production of more precise and highly reproducible EHTs in large series (See contraction experiments, Fig. 11.12). It also opens the way for a multiwell apparatus for drug screening or target validation. Such a device is presently under construction.

7.2. Tissue Engineering

The replacement of defective cardiac tissue by functioning myocardium offers an exciting option in cardiovascular medicine [Li et al., 1998; Reinlib and Field, 2000]. Two principal strategies have been tested so far, mainly in the cryoinjury

or in the myocardial infarction model after coronary ligation in mice and rats. One approach uses isolated cells [Li et al., 1996, 1999; Taylor et al., 1998; Etzion et al., 2001; Orlic et al., 2001; Koh et al., 1995; Scorsin et al., 1997; Kobayashi et al., 2000; Menasche et al., 2001; Reinecke et al., 1999], the other in vitro designed tissue equivalents [Leor et al., 2000; Li et al., 1999, 2000]. In most studies, injection of cells into the scar tissue improved global heart function. Surprisingly, the effect appeared to be independent of cell origin, because positive results were reported from fetal or neonatal cardiac myocytes, fibroblasts, endothelial cells, smooth muscle cells, skeletal myoblasts, or pluripotent stem cells [Li et al., 1996, 1999; Taylor et al., 1998; Etzion et al., 2001; Orlic et al., 2001; Koh et al., 1995; Scorsin et al., 1997; Kobayashi et al., 2000]. The concept of expanding autologous skeletal myoblasts ex vivo and injecting them into the postinfarction scar during coronary artery bypass grafting has already been transferred to the human, and the first results appear promising except for an apparent potential to induce arrhythmia [Menasche et al., 2001]. Despite survival and differentiation of implanted cells, mechanical and electrical cell-cell contact between graft and host, a chief requirement for synchronous contractions, was only rarely observed in carefully designed studies [Etzion et al., 2001; Reinecke et al., 1999] and, accordingly, the proof of direct participation of the grafted material in overall cardiac contraction is lacking. Formation of scar tissue inhibiting contact between grafted cells and host tissue appears to account for this problem at least partly [Etzion et al., 2001; Reinecke et al., 1999]. Successful implantation of bone marrow-derived stem cells into the infarction scar was reported in mice [Orlic et al., 2001]. According to this study, stem cells acquired a cardiac phenotype at a surprisingly high frequency. If confirmed by others independently, this study is important in demonstrating the principal potential of an autologous adult stem cell approach.

An alternative approach to cell grafting procedures is tissue replacement with in vitro designed cardiac constructs. For in vitro tissue construction several scaffold proteins and synthetically produced polymers have been tested, including collagen, gelatin, alginate, and polyglycolic acid [Eschenhagen et al., 1997; Zimmermann et al., 2000; Carrier et al., 1999; Leor et al., 2000; Li et al., 2000]. There are some principal problems with this approach:

(i) Scaffold materials often exhibit an intrinsic stiffness that may compromise diastolic function.

(ii) Biodegradation of the scaffold materials remains incomplete, adding to the potential problems with diastolic function.

(iii) Size limitations exist for of all 3D engineered constructs. Li and coworkers [2000] reported that cardiac myocytes seeded on or in gelatin meshes formed a 300-μm-thick cell layer only on the outside. Bursac and coworkers [1999] observed that cardiac myocytes, when seeded on polymer scaffolds, would form cell layers of 50–70 μm. A homogeneous cell distribution within the constructs was not achieved by either group. Core ischemia is well known

in papillary muscles with diameters >100 μm [Schouten and ter Keurs, 1986; Gülch and Ebrecht, 1987]. In rat hearts the intercapillary distance is 17–19 μm [Korecky et al., 1982].

EHTs have some principal advantages and share some of these problems. In our view, the advantages are the clearly longitudinally oriented, well-coupled network of muscle bundles, the remarkable degree of differentiation, a cardiac tissue-like contractile function including very low resting tension, and the organoid nature of the construct with a surface lining consisting of nonmyocytes and capillarization. These features should prove advantageous for survival, vascularization, and synchronous beating with the host myocardium. In addition, core ischemia is unlikely because the compact muscle bundles with a diameter of 30–100 μm (See Fig. 6a) were found throughout the EHTs without preferential formation at the outer layers. This indicates that the collagen matrix at the concentration used in this study does not represent a significant diffusion barrier or, alternatively, is rapidly degraded.

However, important limitations remain:

1. The cardiac tissue-like network in EHTs is (with the exception of the compact strands, See Fig. 11.6a, Color Plate 6D) generally much less compact than in native tissues (See Figs. 11.7, Color Plate 6E and 11.8, Color Plate 6F), explaining why contractile force is, in absolute terms, about 10-fold less than in comparable intact cardiac preparations. Very thin cardiac muscle preparations develop maximal twitch tension of >20 mN/mm^2 in ferret, rat, cat, rabbit, and human [Holubarsch et al., 1996]. In contrast, maximal forces in EHTs amounted to 2 mN/EHT, that is, 2 mN/mm^2.
2. The degree of cardiac differentiation, despite being superior to 2D cultures (e.g., T-tubules, SR junctions), is clearly less than in intact adult myocardium (e.g., no mature M-bands).
3. The compact musclelike strands (See Fig. 11.6a, Color Plate 6D) did not exceed 30–100 μm in diameter, which is in line with theoretical considerations and published data. Possibly, optimized culture conditions could allow for thicker and more compact EHTs.
4. Finally, and most importantly, it is unknown at present whether EHTs indeed can serve as a tissue equivalent for replacement therapy and have advantages over cell grafting approaches. These questions are currently under investigation [Zimmermann et al., 2002b].

ACKNOWLEDGMENTS

This study was supported by the German Research Foundation (Deutsche Forschungsgemeinschaft) to T. E. (Es 88/8-2) and the German Ministry for Education and Research to T. E. and W. H. Z. (BMBF FKZ 01GN 0124). We greatly appreciated the support from Prof. W. Neuhuber with electron microscopy and

Drs. G. Wasmeier and U. Nixdorff with echocardiography and the excellent technical assistance of B. Endress, A. Hilpert, and I. Zimmermann, Erlangen. Parts of this study were components of the doctoral theses performed by P. Schubert, K. Schneiderbanger, M. Didié, and I. Melnychenko at the University of Erlangen-Nuremberg.

SOURCES OF MATERIALS

Item	*Supplier*
Antibiotics	Biochrom AG
BMON software	Ingenieurbüro Jäckel
Bovine serum albumin	Sigma
Chick embryo extract	CVSciences
2,3-Butanedione monoxime (BDM)	Sigma
Collagen I from rat tails	CVS GmbH
Confocal microscope	Zeiss
DMEM	Biochrom AG
DNase II, Type V from bovine spleen	Sigma
Epon	Roth
Fetal calf serum	Biochrom AG
Force transducer	Ingenieurbüro Jäckel
Glutamine	Biochrom AG
Glutaraldehyde	Roth
Harbor Extracellular Matrix	Harbor Bio-Products/Tebu
Horse serum	Invitrogen
Inorganic salts and HEPES	Merck
Liquid silicone glue	Dow Corning
Matrigel	BD Biosciences
Osmium tetroxide	Roth
PBS	Invitrogen/GIBCO
Petri dishes, 15 cm, Falcon 3000	BD Biosciences
Thimerosal	Sigma
Tris•HCl	Sigma
Triton X-100	Sigma
Trypsin, certified 1:250 crude	Difco, See Becton Dickinson
Ultramicrotome, Ultracut UCT	Leica
Vibratome slicer	Campden Instruments

REFERENCES

Akins, R.E., Boyce, R.A., Madonna, M.L., Schroedl, N.A., Gonda, S.R., McLaughlin, T.A., Hartzell, C.R. Cardiac organogenesis in vitro: reestablishment of three-dimensional tissue architecture by dissociated neonatal rat ventricular cells. *Tissue Eng.* (1999) 5: 103–118.

Anversa, P., Olivetti, G., Bracchi, P.G., Loud, A.V. (1981) Postnatal development of the M-band in rat cardiac myofibrils. *Circ. Res.* 48: 561–568.

Bishop, S.P., Anderson, P.G., Tucker, D.C. (1990) Morphological development of the rat heart growing in oculo in the absence of hemodynamic work load. *Circ. Res.* 66: 84–102.

Bursac, N., Papadaki, M., Cohen, R.J., Schoen, F.J., Eisenberg, S.R., Carrier, R., Vunjak-Novakovic, G., Freed, L.E. (1999) Cardiac muscle tissue engineering: toward an in vitro model for electrophysiological studies. *Am. J. Physiol. Heart Circ. Physiol.*;277: H433–H444.

Carrier, R.L., Papadaki, M., Rupnick, M., Schoen, F.J., Bursac, N., Langer, R., Freed, L.E., Vunjak-Novakovic, G. (1999) Cardiac tissue engineering: cell seeding, cultivation parameters, and tissue construct characterization. *Biotechnol. Bioeng.*64: 580–589.

Communal, C., Huq, F., Lebeche, D., Mestel, C., Gwathmey, J.K., Hajjar, R.J. (2003) Decreased efficiency of adenovirus-mediated gene transfer in aging cardiomyocytes. *Circulation* 107: 1170–1175.

Condorelli, G., Borello, U., De Angelis, L., Latronico, M., Sirabella, D., Coletta, M., Galli, R., Balconi, G., Follenzi, A., Frati, G., Cusella De Angelis, M.G., Gioglio, L., Amuchastegui, S., Adorini, L., Naldini, L., Vescovi, A., Dejana, E., Cossu, G. (2001) Cardiomyocytes induce endothelial cells to trans-differentiate into cardiac muscle: implications for myocardium regeneration. *Proc. Natl. Acad. Sci. USA* 98: 10,733–10,738.

El-Armouche, A., Rau, T., Zolk, O., Ditz, D., Pamminger, T., Zimmermann, W.H., Jäckel, E., Harding, S.E., Boknik, P., Neumann, J., Eschenhagen, T. (2003) Evidence for protein phosphatase inhibitor-1 playing a positive feedback role in β-adrenergic signaling in cardiac myocytes. *FASEB J.* 17: 437–439

Eschenhagen, T., Fink, C., Remmers, U., Scholz, H., Wattchow, J., Weil, J., Zimmermann, W.H., Dohmen, H.H., Schäfer, H.J., Bischopric, N., Wakatsuki, T., Elson, E.L. (1997) Three dimensional reconstitution of embryonic cardiomyocytes in a collagen matrix: a new heart muscle model system. *FASEB J.* 11: 683–694.

Eschenhagen, T., Didié, M., Münzel, F., Schubert, P., Schneiderbanger, K., Zimmermann, W.H. (2002) 3D engineered heart tissue for replacement therapy. *Basic Res. Cardiol.* 2002(Suppl 1): I146–I152

Etzion, S., Battler, A., Barbash, I.M., Cagnano, E., Zarin, P., Granot, Y., Kedes, L.H., Kloner, R.A., Leor, J. (2001) Influence of embryonic cardiomyocyte transplantation on the progression of heart failure in a rat model of extensive myocardial infarction. *J. Mol. Cell. Cardiol.* 33: 1321–1330.

Fechner, H., Noutsias, M., Tschoepe, C., Hinze, K., Wang, X., Escher, F., Pauschinger, M., Dekkers, D., Vetter, R., Paul, M., Lamers, J., Schultheiss, H.P., Poller, W. (2003) Induction of coxsackievirus-adenovirus-receptor expression during myocardial tissue formation and remodeling: identification of a cell-to-cell contact-dependent regulatory mechanism. *Circulation* 107: 876–882.

Fink, C., Ergün, S., Kralisch, D., Remmers, U., Weil, J., Eschenhagen, T. (2000); Chronic stretch of engineered heart tissue induces hypertrophy and functional improvement. *FASEB J.* 14: 669–679.

Gülch, R.W., and Ebrecht, G. (1987) Mechanics of rat myocardium revisited: investigations of ultra-thin cardiac muscles under high energy demand. *Basic Res. Cardiol.* 82 Suppl 2: 263–274.

Holubarsch, C., Ruf, T., Goldstein, D.J., Ashton, R.C., Nickl, W., Pieske, B., Pioch, K., Ludemann, J., Wiesner, S., Hasenfuss, G., Posival, H., Just, H., Burkhoff, D. (1996) Existence of the Frank-Starling mechanism in the failing human heart. *Circulation* 94: 683–689.

Katz, A.M. (1992) Structure of the heart. In: *Physiology of the Heart*, 2nd ed, New York, NY, Raven Press, pp. 1–36.

Kilborn, M.J., and Fedida, D. (1990) A study of the developmental changes in outward currents of rat ventricular myocytes. *J. Physiol.* 430: 37–60

Kobayashi, T., Hamano, K., Li, T.S., Katoh, T., Kobayashi, S., Matsuzaki, M., Esato, K. (2000) Enhancement of angiogenesis by the implantation of self bone marrow cells in a rat ischemic heart model. *J. Surg. Res.* 89: 189–195.

Koh, G.Y., Soonpaa, M.H., Klug, M.G., Pride, H.P., Cooper, B.J., Zipes, D.P., Field, L.J. (1995) Stable fetal cardiomyocyte grafts in the hearts of dystrophic mice and dogs. *J. Clin. Invest.* 96: 2034–2042.

Koh, G.Y., Soonpaa, M.H., Klug, M.G., Field, L.J. (1993) Long-term survival of AT-1 cardiomyocyte grafts in syngeneic myocardium. *Am. J. Physiol. Heart Circ. Physiol.* 264: H1727–H1733.

Kolodney, M.S., and Elson, E.L. (1993) Correlation of myosin light chain phosphorylation with isometric contraction of fibroblasts. *J. Biol. Chem.* 268: 23,850–23,855.

Korecky, B., Hai, C.M., Rakusan, K. (1982) Functional capillary density in normal and transplanted rat hearts. *Can. J. Physiol. Pharmacol.* 60: 23–32.
Kostin, S., Scholz, D., Shimada, T., Maeno, Y., Mollnau, H., Hein, S., Schaper, J. (1998) The internal and external protein scaffold of the T-tubular system in cardiomyocytes. *Cell Tissue Res*. 294: 449–460.
Kostin, S., Klein, G., Szalay, Z., Hein, S., Bauer, E.P., Schaper, J. (2002) Structural correlate of atrial fibrillation in human patients. *Cardiovasc. Res.* 54: 361–379.
Leor, J., Aboulafia-Etzion, S., Dar, A., Shapiro, L., Barbash, I.M., Battler, A., Granot, Y., Cohen, S. (2000) Bioengineered cardiac grafts: A new approach to repair the infracted myocardium? *Circulation*. 102: III56–III61.
Li, R.K., Mickle, D.A., Weisel, R.D., Zhang, J., Mohabeer, M.K. (1996) In vivo survival and function of transplanted rat cardiomyocytes. *Circ. Res.* 78: 283–288
Li, R.K., Jia, Z.Q., Weisel, R.D., Merante, F., Mickle, D.A. (1999) Smooth muscle cell transplantation into myocardial scar tissue improves heart function. *J. Mol. Cell. Cardiol.* 31: 513–522.
Li, R.K., Yau, T.M., Sakai, T., Mickle, D.A., Weisel, R.D. (1998) Cell therapy to repair broken hearts. *Can. J. Cardiol.* 14: 735–744.
Li, R.K., Yau, T.M., Weisel, R.D., Mickle, D.A., Sakai, T., Choi, A., Jia, Z.Q. (2000) Construction of a bioengineered cardiac graft. *J Thorac. Cardiovasc. Surg.* 119: 368–375.
Menasche, P., Hagege, A.A., Scorsin, M., Pouzet, B., Desnos, M., Duboc, D., Schwartz, K., Vilquin, J.T., Marolleau, J.P. (2001) Myoblast transplantation for heart failure. *Lancet*. 357: 279–280.
Mende, U., Eschenhagen, T., Geertz, B., Schmitz, W., Scholz, H., Schulte am Esch, J., Sempell, R., Steinfath, M. (1992) Isoprenaline-induced increase in the 40/41 kDa pertussis toxin substrates and functional consequences on contractile response in rat heart. *Naunyn Schmiedebergs Arch. Pharmacol.* 345: 44–50.
Most, P., Bernotat, J., Ehlermann, P., Pleger, S.T., Reppel, M., Borries, M., Niroomand, F., Pieske, B., Janssen, P.M., Eschenhagen, T., Karczewski, P., Smith, G.L., Koch, W.J., Katus, H.A., Remppis, A. (2001) S100A1: a regulator of myocardial contractility. *Proc. Natl. Acad. Sci. USA* 98: 13,889–13,894.
Müller-Ehmsen, J., Peterson, K.L., Kedes, L., Whittaker, P., Dow, J.S., Long, T.I., Laird, P.W., Kloner, R.A. (2002a) Rebuilding a damaged heart: long-term survival of transplanted neonatal rat cardiomyocytes after myocardial infarction and effect on cardiac function. *Circulation* 105: 1720–1726.
Müller-Ehmsen, J., Whittaker, P., Kloner, R.A., Dow, J.S., Sakoda, T., Long, T.I., Laird, P.W., Kedes, L. (2002b) Survival and development of neonatal rat cardiomyocytes transplanted into adult myocardium. *J. Mol. Cell. Cardiol.* 34: 107–116.
Orlic, D., Kajstura, J., Chimenti, S., Jakoniuk, I., Anderson, S.M., Li, B., Pickel, J., McKay, R., Nadal-Ginard, B., Bodine, D.M., Leri, A., Anversa, P. (2001) Bone marrow cells regenerate infarcted myocardium. *Nature* 410: 701–705.
Reinecke, H., Zhang, M., Bartosek, T., Murry, C.E. (1999) Survival, integration, and differentiation of cardiomyocyte grafts: a study in normal and injured rat hearts. *Circulation* 100: 193–202.
Reinlib, L., and Field, L. (2000) Cell transplantation as future therapy for cardiovascular disease?: A workshop of the National Heart, Lung, and Blood Institute. *Circulation* 101: E182–E187.
Remppis, A., Pleger, S.T., Most, P., Lindenkamp, J., Ehlermann, P., Schweda, C., Löffler, E., Weichenhan, D., Zimmermann, W.H., Eschenhagen, T., Koch, W.J., Katus, H.A. (2004) S100A1 gene transfer: A strategy to strengthen engineered cardiac grafts. *J. Gene Med.* 6(4): 387–394.
Roell, W., Lu, Z.J., Bloch, W., Siedner, S., Tiemann, K., Xia, Y., Stoecker, E., Fleischmann, M., Bohlen, H., Stehle, R., Kolossov, E., Brem, G., Addicks, K., Pfitzer, G., Welz, A., Hescheler, J., Fleischmann, B.K. (2002) Cellular cardiomyoplasty improves survival after myocardial injury. *Circulation* 105: 2435–2441.
Sakai, T., Li, R.K., Weisel, R.D., Mickle, D.A., Jia, Z.Q., Tomita, S., Kim, E.J., Yau, T.M. (1999) Fetal cell transplantation: a comparison of three cell types. *J. Thorac. Cardiovasc. Surg.* 118: 715–724.

Schouten, V.J., and ter Keurs, H.E. (1986) The force-frequency relationship in rat myocardium. The influence of muscle dimensions. *Pflügers Arch*. 407: 14–17.
Scorsin, M., Hagege, A., Vilquin, J.T., Fiszman, M., Marotte, F., Samuel, J.L., Rappaport, L., Schwartz, K., Menasche, P. (2000) Comparison of the effects of fetal cardiomyocyte and skeletal myoblast transplantation on postinfarction left ventricular function. *J. Thorac. Cardiovasc. Surg.* 119: 1169–1175.
Soonpaa, M.H., Koh, G.Y., Klug, M.G., Field, L.J. (1994) Formation of nascent intercalated disks between grafted fetal cardiomyocytes and host myocardium. *Science* 264: 98–101.
Souren, J.E.M., Schneijdenberg, C., Verkeleij, A.J., Van Wijk, R. (1992) Factors controlling the rhythmic contraction of collagen gels by neonatal heart cells. *In Vitro Cell Dev. Biol.* 28A: 199–204.
Taylor, D.A., Atkins, B.Z., Hungspreugs, P., Jones, T.R., Reedy, M.C., Hutcheson, K.A., Glower, D.D., Kraus, W.E. (1998) Regenerating functional myocardium: improved performance after skeletal myoblast transplantation. *Nat. Med.* 4: 929–933.
Tomita, S., Li, R.K., Weisel, R.D., Mickle, D.A., Kim, E.J., Sakai, T., Jia, Z.Q. (1999) Autologous transplantation of bone marrow cells improves damaged heart function. *Circulation* 100: II247–II256.
Webster, K.A., Discher, D.J., Bishopric, N.H. (1994) Regulation of fos and jun immediate-early genes by redox or metabolic stress in cardiac myocytes. *Circ. Res.* 74: 679–686
Weil, J., Eschenhagen, T., Hirt, S., Magnussen, O., Mittmann, C., Remmers, U., Scholz, H. (1998) Preserved Frank-Starling mechanism in human end stage heart failure. *Cardiovasc. Res.* 37: 541–548.
Zimmermann, W.H., Fink, C., Kralisch, D., Remmers, U., Weil, J., Eschenhagen, T. (2000) Three-dimensional engineered heart tissue from neonatal rat cardiac myocytes. *Biotechnol. Bioeng.* 68: 106–114.
Zimmermann, W.H., Schneiderbanger, K., Schubert, P., Didié, M., Münzel, F., Heubach, J.F., Kostin, S., Neuhuber, W.L., Eschenhagen, T. (2002a) Tissue engineering of a differentiated cardiac muscle construct. *Circ. Res.* 90: 223–230.
Zimmermann, W.H., Didié, M., Wasmeier, G.H., Nixdorff, U., Hess, A., Melnychenko, I., Boy, O., Neuhuber, W.L., Weyand, M., Eschenhagen, T. (2002b) Cardiac grafting of engineered heart tissue. *Circulation* 106: I151–I157.
Zimmermann, W.H., Melnychenko, I., Eschenhagen, T. (2004) Engineered heart tissue for regeneration of diseased hearts. *Biomaterials* 25(9): 1639–1647.
Zimmermann, W.H., Melnychenko, I., Wasmeier, G., Nixdorff, U., Michaelis, B., Dhein, S., Budensky, L., Hess, A., Eschenhagen, T. (2003) Gewebeersatztherapie nach transmuralem Myokardinfarkt. *Z. Kardiol.* 92: I/243 (abstract).
Zolk, O., Marx, M., Jackel, E., El-Armouche, A., Eschenhagen, T. (2003) β-Adrenergic stimulation induces cardiac ankyrin repeat protein expression: involvement of protein kinase A and calmodulin-dependent kinase. *Cardiovasc. Res.* 59: 563–572.